Development of an alarming system for an unmanned railway crossing using vibration transmission in railway track

A Dissertation

submitted in partial fulfilment of requirements for the degree of

Master of Engineering

In

CAD/CAM Engineering

by

Sanjay Thakur

Registration no.- 801784016

Under the supervision of

Dr. Ashish Purohit

Assistant Professor

Mechanical Engineering Department

MECHANICAL ENGINEERING DEPARTMENT

THAPAR INSTITUTE OF ENGINEERING AND TECHNOLOGY

PATIALA, PUNJAB

JULY 2019

CERTIFICATE

This is to certify that the work done in this thesis title "**Development of an alarming system for an unmanned railway crossing using vibration transmission in railway track"** submitted in the partial fulfilment of requirement for the award of Master of Engineering degree in CAD/CAM in the mechanical engineering department of Thapar Institute of Engineering and Technology, Patiala, is an authentic record of the work carried out by me under the guidance of Dr. Ashish Purohit, Mechanical Engineering Department, Thapar Institute of Engineering and Technology, Patiala. The embodied in this report has not been submitted in any part or full to any other university or institute for the award of any degree.

Sanjay Thakur

Roll no. 801784016

This is to certify that above declaration made by the student concerned is corrected to the best of my knowledge and belief.

Dr. Ashish Purohit

Assistant Professor,

MED

Dated: 05-08-2019

ACKNOWLEDGEMENT

Foremost, I would like to express my sincere gratitude to my Advisor Asst. Prof. Dr. Ashish Purohit for the continuous support of ME study and research, for his motivation, enthusiasm, and immense knowledge. The door to Prof. Purohit's office was always open whenever I ran into trouble and asked any question about my research. His guidance helped me during the time of research and writing this thesis. I have learned so much from him and looking forward to his continuous support for future endeavours in life.

Finally, I must express my very profound gratitude to my parents for providing me with constant support and continuous encouragement throughout my year of my study and during the process of research and writing the thesis. This accomplishment would not have been possible without them.

ABSTRACT

In present work, a finite element model of railway track having fish plate joint is developed to study the vibration transmission characteristics of the railway track and fish plate joint when vibration transmitted through it. Numerical simulation of FE model has been done in a commercial tool ANSYS Workbench. In railway tracks, there must be gaps between two tracks for expansion of the rails. A fish plate joint is used to join both the ends of the joint. Unmanned railway crossings across the country is a major concern of safety and hence, it is important to provide an automated alarming mechanism which can sense the arrival of train. Vibration of the track can be used to sense the arrival of train. But there are number of fish plate joints in the railway track and it is important to study the role of the joint in vibration transmission. Hence, a model having multiple tracks have been designed to identify the effect of fish plate joint in transmission of vibration. A small-scale test model has also been developed to validate the accuracy of the results obtained in the ANSYS by comparing the natural frequency of the model with experimental test setup. It is concluded from the present work that, there is very less decay in the vibration signal when it passes through the joint and hence joint may be neglected for further dynamic study in railway tracks. The distance at which we can get the genuine vibration signal is calculated as 85 meters. So, the vibration sensing device used to sense the vibration signal must be put within this distance.

CONTENTS

LIST OF FIGURES

LIST OF TABLES

NOMENCLATURES AND ABBREVIATIONS

L	Length of track.
a	Distance between sleepers.
b	Distance between sleepers at rail joint.
d	Gap between rails.
c	Damping of the spring.
k	Stiffness of the spring.
Hz	Hertz.
E	Elastic modulus.
I	Moment of inertia.
w	Deflection of beam.
μ	Mass per unit length.
q	Applied force.
F	Force applied.
N	Newton

IRJ	Insulated Rail Joint
FEM	Finite Element Method

CHAPTER 1

INTRODUCTION

1.1 Scope of the work:

In India, there are many unmanned railways crossings across the country, which is a big concern from the safety point of view. There is no flagman or any other safety precaution in unmanned railway crossings which prevent any vehicles or human for crossing the path of the coming train. In India, these level crossings account for 40% of train accidents and 60% of casualties due to man crossing. Hence, it is important to provide an automated alarming mechanism which senses the arrival of train when train is at some distance from the crossing. In the present state, for the manned railway crossings, a person is deployed to control the closing and opening of the crossing. For this purpose, a wired signalling system is used. In case of an unmanned crossing, such system cannot be worked as a person is required to execute the closing and opening operation. Therefore, an automated system, which can sense arrival of train in well advance and prompt alarm, is demanded.

When train runs over rails, it produces high dynamic impact forces. These impact forces lead to vibration in the track. Vibration in the track can be used to sense the arrival of the train at unmanned railway crossings and then give active alarm at the crossing. Development of such alarming system essentially required to study the vibration carrying characteristics of the railway tracks. It may be noted that, in the railway tracks, there must be a gap between two rails for the expansion of the rails in hot days and suitable joints are employed for joining of two rails with each other and also line up the ends of rails for smooth running of wheels over

rail. Fish plate is the commonly used rail joint which is tightened between the two ends of the rails with the help of bolts.

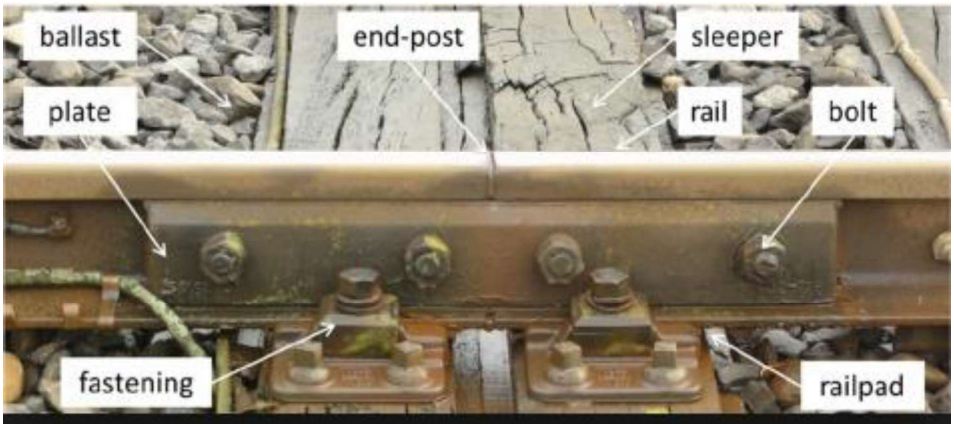

Fig. 1 Components of rail joint (Oregui et al. 2015)

In railway track, after every 10-12 m distance, a fish plate joints are placed. The design and the components of rail joint is shown in Fig. 1 (Oregui et al. 2015). These fish plate joints may affect the vibration transmission through rails and thus, in addition to find the vibration transmission characteristics of the track, it is also important to study the vibration transmission characteristics of a fish plate joint. From the literature, it is observed that in most of the previous work related to analysis of railway tracks, their health against the heavy loads subjected from the wagons are investigated. In other studies of modelling and analysis of fish plate joint, the focus of the study was mainly to identify strength of the joint, dynamic analysis of fish plate joint is rare. Particularly, study to identify vibration transmission characteristics of fish plate joint is absent.

Therefore, to calculate the vibration transmission characteristics of a railway track, dynamic analysis of both the rails and fish plate joints are equally important. The objective of the present study is two folds. The primary goal of the present work is to correct modelling and dynamic analysis of fish plate joint including contact nature of the joint. Secondary objective of the study is to know the vibration transmission nature of a railway track including joints. In our

study, all the analyses are performed on a finite element bases commercial tool ANSYS workbench. As a test model, a three-dimensional model consist of fish plates and long tracks at both the sides of the joint plate is developed and simulated for different excitation conditions. An infinite long track is infeasible to model therefore, suitable boundary conditions are implemented. In this study, different models having different number of rails have been designed for studying the decay in vibration signal throughout the railway track and effect of joint in vibration signal transmission. Pang and Dhanasekar (2006) shows the cross section of the rail joint.

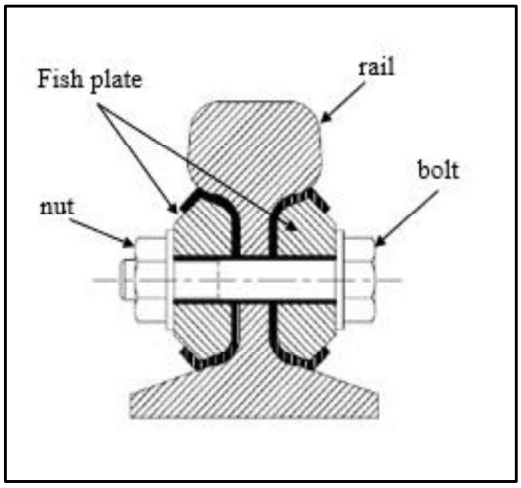

Fig. 2 Cross section of the rail joint (Pang and Dhanasekar 2006)

1.2 Thesis outline:

Chapter 1 describes the motivation and the scope of present thesis work which is "Development of an alarming system for an unmanned railway crossing using vibration transmission in railway track". This chapter also includes the need, reason and process of present thesis work. Chapter 2 describes the literature study which I have done to obtain the useful information and data related to my thesis. This chapter also discussed about the gaps and objectives of present work. Chapter 3 describes the methodology, model formulation and any assumptions made

during the model formulation. This chapter describes the theoretical formulation used in the present work. Numerical modelling is also described in this chapter. This chapter includes all the steps used to obtain the desired model and all the assumptions used in numerical simulation. Experimental procedure is also included in this chapter. Chapter 4 includes the results obtained from numerical simulation. This chapter includes all the graphs and tabular data which is obtained from the simulation. Chapter 5 describes the conclusions of thesis and future scope of present work.

CHAPTER 2

LITERATURE REVIEW

In several literatures, different types of analysis and study has been done on fish plate joint. The various experimental and numerical analysis has been performed for identifying different parameters of fish plate joint. The literature survey has been done and is given below:

2.1 Study of health condition of rail joint:

Gallou et al. (2018) have investigated different ways of reducing failure and deterioration of rail joint. In this paper, a static FEM model is designed to numerically simulate the dynamics of rail joint. Different support stiffnesses are used to compare the plain rail and rail joint. Results of model are compared with field data taken by Video-Gauge, which is an optical measurement instrument. It has been obtained from the results that the use of I-beam section and strap rails at rail joint provides more stiffness to the support and hence decreasing the displacement at the rail joint.

Gallou (2018) have presented a paper in which performance of rail joint is studied. An experiment is performed on railway track in which Video Gauge is used to assess the deflection in track and stiffness of supports at track site. It is concluded that a Video Gauge can directly be used for assessing the condition of rail joint. It is also observed that variable of deflection in track and track stiffness can be caused by varying the dynamic loading.

Mandal and Peach (2010) have presented an engineering analysis of different designs of insulated rail joint and failure of the IRJ. A 3D finite element model has been used for different joint bar sizes and analysing the stresses formed in joint bars. It has been concluded that to increase the bending stiffness of the bar, height of the bar should be increased instead of the thickness of the bar to decrease the displacement and the stresses at rail joint.

Mandal (2014) have presented a finite element model to reduce the fatigue failure at the railhead of the insulated rail joint. Numerical simulation has been carried out on railhead material in which dynamic wheel load has been applied. Von-Mises stresses and residual stresses has been analysed for determining metal flow across rail joint. It is noted from the results that the depth of the plastic zone on the railhead material is 8mm in to sub-surface layer.

Oregui et al. (2015) have performed an experiment for investigating the condition of the rail joint when impact excitation has been applied on it. Three conditions have been analysed for monitoring IRJ i.e., Broken fastening, damaged insulated layer and railhead having plastic deformation. A hammer test has been performed on the rail joint for determining feasibility of the model. It has been found from the results that damaged joint differed significantly from the reference rail joint in measured high frequency range.

Patel et al. (2013) have estimated the fatigue life of Insulated Rail Joint for inspection interval selection of the rail joint. A 3-D numerical model has been proposed and static and dynamic loading were being applied for estimation of the fatigue life of the joint and strength at the joint. The ends of model have been taken as free for the simulation. Tensile bending stress has been calculated at the rail head for calculation of crack growth. It has been observed from the results that engineering analysis of rail joint provides estimation of fatigue for vertical bending only.

Sandstrom and Ekberg (2009) have presented a paper in which numerical study has been done to determine the plastic deformation and fatigue failure of rail joint. It has been found that due to the longitudinal loading at the rail joint the rail degrades at the region of rail joint. Fatigue impact was measured at three different positions and the magnitude of strain was found so high at the railhead edge.

Zong and Dhanasekar (2017) have presented a paper in which the new design of IRJ has been modelled for minimising different failures in the joint. Sleeper embedded rail joint has been modelled in numerical simulation. It has been observed from the results that cracking of joint bar and loosening or cracking of bolts can all be minimised in new sleeper embedded rail joint.

2.2 Study of wheel-rail interaction:

Cai et al. (2007) have developed a model for analysis of using finite element analysis for rail joint with height difference defect. In this model, the ends of rails are taken as free so as to prevent the wave reflections of stress generated at the boundary. Contact elements are also used for interaction between rail-wheel and rail-joint. The effect of speed of train and load of axle with height difference on contact forces are investigated at rail top. It is observed that the speed of train has more effect on contact forces than the load of axle.

Chen and Kuang (2002) have presented a paper in which contact stress variation near rail joint is simulated using FE models. Elastic IRJ materials are used for numerical simulation. In this paper, it is concluded that IRJ might affect the contact stress distribution. It is also observed from the literature that Hertzian contact is no longer available for stress distribution at rail joint region.

Clarke et al. (1982) have presented a paper in which a model is developed to investigate the dynamic model of vehicle running on rails. In this research, rail ends are taken as fixed so that they neither deflect nor rotate. A mathematical model is developed in this paper to study the dynamics of rail-wheel. An experiment is also performed to verify the theoretical results. It is observed from the study that rail vibrates out of phase on different frequencies considering corrugation of rails.

Dong et al. (1994) have developed a FE model to study the dynamic behaviour between wheel and rail. Dynamic forces on track is measured and strain on railway track is calculated from the model. The impact load at constant speed is provided to the rail and steady state response of system is calculated and compared with the experimental results. It is concluded from the research that the load of axle and the speed of train are the important factors which affects the wheel rail impact most and the force exerted on the system is mostly affected by the stiffness of rail pad and mass of tie.

Grassie et al. (1982) have presented 2 models of railway track having different sleepers. Two types of sleepers used in this paper for modelling i.e. wooden sleepers and concrete sleepers. These models are used to obtain contact force between wheel and rail. The response for both the sleepers and effect of rail pads are also included in this research. It is concluded that in concrete sleepers the magnitude of force generated on contact is dependent on the stiffness of rail pad whereas in wooden sleepers, the sleeper vibration on rail pad has not been observed.

Hasna (2015) have presented a finite element model to study the dynamic behaviour of the rail joint. The support stiffness and dynamic forces on wheel-rail has been studied. Equivalent stress and vertical displacement of rail for different soil conditions has been measured. The

result shows that on loose sand the displacement is maximum and on very high graded dense sand, the displacement is minimum.

Himebaugh et al. (2008) have presented a paper in which a finite element analysis is performed on bonded Insulated Rail Joint. A numerical simulation has been performed in which static wheel load is applied to the model and rails are also subjected to tensile load. The vertical deflection and the shear stresses at rails are determined. It is observed from the results that if size of joint is increased, the maximum shear stress decreased and if thickness of joint increased, the maximum shear stress also increased significantly.

Kerr and Cox (1999) have presented a paper in which different tests are conducted on rail joint and analytical formulation is also done on bonded insulated rail joint. Numerical analysis is also performed for rail joint. Static load is applied on the joint and verified the data with test results. It is observed from the results that if repetitive loads are applied for long duration at the joint then delamination between rail and joint may take place and due to this, larger deflections can take place at joint region.

Lal et al. (2016) have presented a numerical model for analysing the stresses at wheel-rail contact region. A wheel-rail model was simulated and contact stresses at rail has been identified. Static analysis was used and wheel load was applied in vertical downward direction. Stresses for different types of rails has been determined and then compared. It has been noted from the results that maximum contact stress at rail wheel is less than the limiting value of the contact stress.

Nielsen (2008) have presented a paper in which wheel-track interaction is numerically simulated at high frequencies for validation of simulation tool named DIFF. Validation of

numerical model has been done by referring the results of two field tests. The simulation has been carried out for frequency range between 20 Hz to 2000 Hz and the end boundary condition has been taken as fixed for both the ends of rail. It has been obtained from the results that rail pads and ballast are important factors for track dynamics at low frequencies. It has been concluded that a tool used for simulation i.e. DIFF is useful for investigating interaction between wheel and rail at high frequency.

Ono and Yamda (1989) have developed analytical formulation for estimating the vibration generated in the railway track due to the unevenness of the track. The elasticity and mass of material of the track has been taken into consideration. Vibration velocities for the sleepers and roadbed has been identified. Analytical results were compared with the field test results. It has been observed from the study that if rail is supported by resilient rail pads then three kind of vibration is generated in the track and if rail is supported by stiffest rail pads then only one kind of vibration is generated.

Oregui et al. (2012) have proposed a finite element model for investigating the relation between bolt tightness and wheel-track contact. The numerical model is only valid for the frequency range between 150 to 800 Hz. The model has been validated for different damage conditions in the rail joint. From the results, it has been noted that bolt tightness majorly affects the contact force between wheel and rail and the effect of wheel speed is also significant on the wheel-track contact.

Pang and Dhanasekar (2006) have proposed a 3-D finite element model for wheel-rail contact at the Insulated Rail Joint. Contact impact force and pressure distribution at rail joint has been identified. It has been observed that pressure distribution at the contact region is significantly

different for the region away from the contact. If contact patch is nearby the rail joint then IRJ plays an important role in pressure distribution.

Plaut et al. (2007) have investigated a tapered bonded joint to reduce the stresses at rail joint region. Approximate solutions have been obtained from the first type of analysis in which rail and joint bars were considered as a beam. Numerical simulation for finite element model has been used for second type of analysis for determining deflections, stresses and bending moments. It has been noted from the results that in tapered bonded joint the value of deflection, shear stress and bending moment is smaller than the conventional rail joint.

Suzuki et al. (2005) have proposed a track model in which dynamic behaviour at rail joint is considered when wheel passing over the joint. Numerical simulation results then compared with the analytical results. It is observed that joint gaps excite the wheel load at very high frequencies and the values of dynamic wheel load and seat forces around IRJ do not change linearly.

Vyas and Gupta (2006) have presented a paper in which modelling of the dynamics of rail wheel and flat has been done. Wheel flats are the flats on the wheel which provide forces from the wheels four times more than that of normal wheel. A finite element model has been modelled for dynamics of wheel-flat and rail interaction. It has been observed from the analysis that the magnitude of impact on the rail with wheel flats is almost double of the rolling force.

Wen et al. (2004) have developed a finite element model to analyse the wheel-rail impact behaviour. Numerical simulation has been carried out in Ansys in which the effect of wheel load and speed of train on joint is investigated for different parameters. Free boundary condition has been implemented on both ends. In this research, it is observed that wheel load

has more effect on different parameters than the train speed during interaction of rail and wheel.

Yang et al. (2017) have performed a numerical and experimental study to identify the wheel-rail impact vibration at the rail joint. Numerical simulation has been carried out for wheel-joint interaction and to simulate the impact vibration at high frequencies. Hammer test was performed on the rail track and the model has been validated by comparing the results of numerical simulation. It is observed from the results that impact vibration may be minimised by controlling the damping the force or by a new design of rail joint or sleepers.

Zakeri et al. (2009) have presented a paper in which study of 2-D infinite element has been done for modelling of railway track for eliminating the boundary condition effects. It has been noted from the results that when infinite beam has been taken as rails, changes in the maximum displacement was non considerable while when boundary conditions are applied, a notable change in displacement has been noted due to the returned waves or reflections.

Zong et al. (2013) have presented a wheel-track interaction model for determining the impact loading and material characterisation of IRJ. A field experiment has also been presented for validation of predicted impact loading. Numerical simulation has been carried out and it has been noted from the simulation that characteristics of joint material have direct effect on the impact forces. Closer the material properties to the rail steel, lesser will be the impact forces.

In various researches all over the world, same model is developed to find out the different analysis on railway track or rail joint. But still there is no valid clarification for the boundary condition of the ends of rails. In various researches, ends are taken as fixed (Clark et al. and Nielsen) or free (Cai et al., Patel and Wen et al.). Hence, it is still a challenging task to identify the correct boundary condition for the model.

2.3 Summary of the literature review:

In literature review, various experimental and numerical study have been evident the dynamic analysis of a track and also of a fish plate joint. Researchers have studied the strength of fish plate joint and in some of the work; wheel rail contact analysis is carried out. Few investigations are devoted to dynamic analysis of rail track. In different research works, different types of joints have been analysed. Various stress analysis and fatigue analysis are also performed in finite element modelling of joint as well as of the rails. However, it is observed that in most of the previous investigations, the focus of the work was either to find the strength of a track and the fish plate joint or estimate check the failure under the static loads. Studies related to finding out vibration transmission characteristics of the tracks as well as the joint are rare in the literature. In addition, it is also observed that in the numerical modelling of the tracks, modelling of boundary conditions is always a challenge. In some of the study, the ends are considered as free boundary condition (Cai et al., Patel and Wen et al.). Conversely, in some study, ends are modelled as fixed boundary (Clark et al. and Nielsen). But, as the actual system is a continuous system, both kinds of boundaries may give approximate results.

CHAPTER 3

OBJECTIVES AND METHODOLOGY

From the literature review, it is noted that there are various researches carried out in which experimental and numerical study have been done on rail joints, however few studies conducted that showed the vibration transmission through the track and the fish plate joint. In particular, estimation of dynamics of track and the fish plate joint in overall transmission of vibration signal is important for designing a signalling system. Dynamic analysis of the track and joint will help to know that how long the signal will travel without significant. Based on the gap identified from the literature and the need analysis of automation of an unmanned railway track, following objectives are considered for the present study:

- Development of an alarming system using estimation of vibration transmission characteristics of a track along with the fish plate joint.
  - Finite element (FE) modelling of railway track
  - FE modelling of Fish plate joint
  - Validation of correctness of FE model (experimental validation)
  - Dynamic analysis of system against rail wheel loading.

From the review of open literature, it is noted that correct modelling of boundary of the ends of the rails is a challenge. Different researchers have modelled it differently as free end boundary or fixed end boundary. The prime objective of the present work is to understand vibration transmission characteristics of a track with joints. Therefore, in the present work, efforts are primarily dedicated to find the vibration signal decay in the track, irrespective to the

modelling of ends. It is expected that for all the kind of end boundaries, the vibration decay will remain identical.

3.1 Numerical Methodology:

A numerical study has been carried out for modelling of railway track with the joint. Finite element approach has been adopted for the numerical simulation. The simulation has been performed on a commercial tool ANSYS Workbench.

Table 1. Material properties of structural steel:

Properties	Value
Density	7850 Kg/m^3
Young's Modulus	200 GPa
Poisson's Ratio	0.3

All the part of model is defined as solid bodies. The material assigned to the model is structural steel. The properties of assigned material are given in Table 1. Fig. 3 shows the dimensions of a 60 Kg rail model designed for the simulation. Rail track is assembled with fish plate joint with the help of nuts and bolts as shown in the Fig. 4

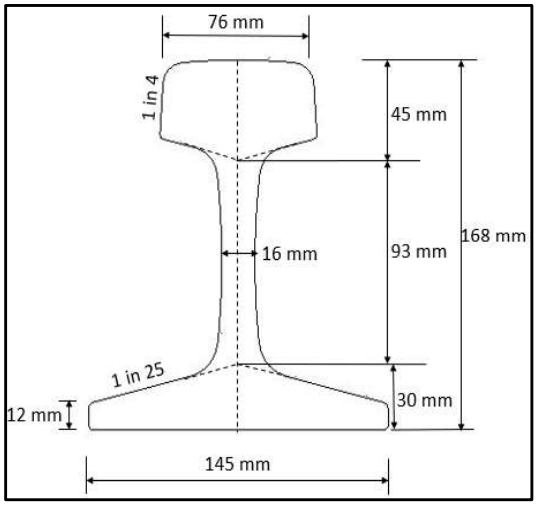

Fig.3 Geometry of 60 Kg rail

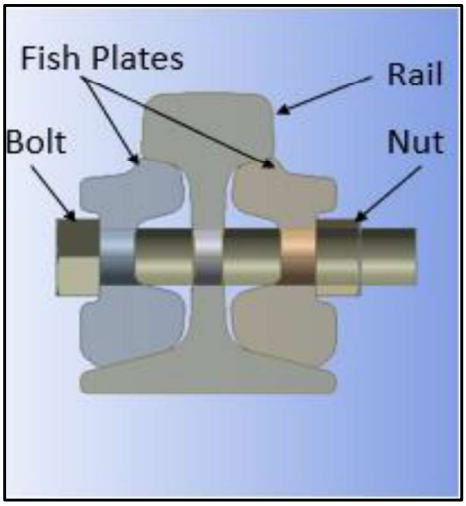

Fig.4 Rail model with fish plate joint

The numerical study involves dynamic forces on the system. For this purpose, Euler Lagrange model has been considered for study the dynamics of the model. The Euler Lagrange equation used for dynamic study is:

$$EI\frac{\partial^4 w}{\partial x^4} = -\mu\frac{\partial^2 w}{\partial x^2} + q \qquad \ldots (1)$$

Where,

E = Elastic modulus

I = Moment of inertia

w = Deflection of beam

μ = Mass per unit length

q = Applied force

The first term of Euler Lagrange equation represents the potential energy due to internal forces (when considered with negative sign) and the second term represents the kinetic energy and the third term represents the potential energy due to external load (q).

3.2 Test Model

The test model consists of two parts, one is rail track and another is fish plate. Transient structural analysis has been done on the test model.

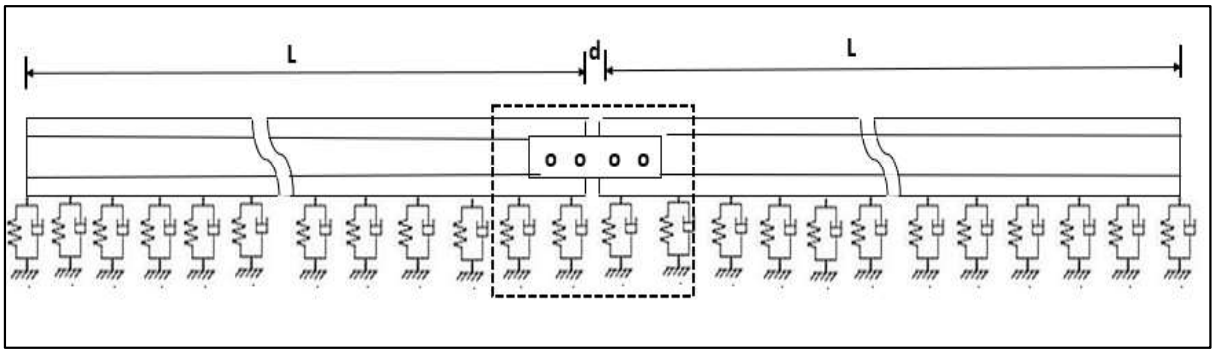

(a)

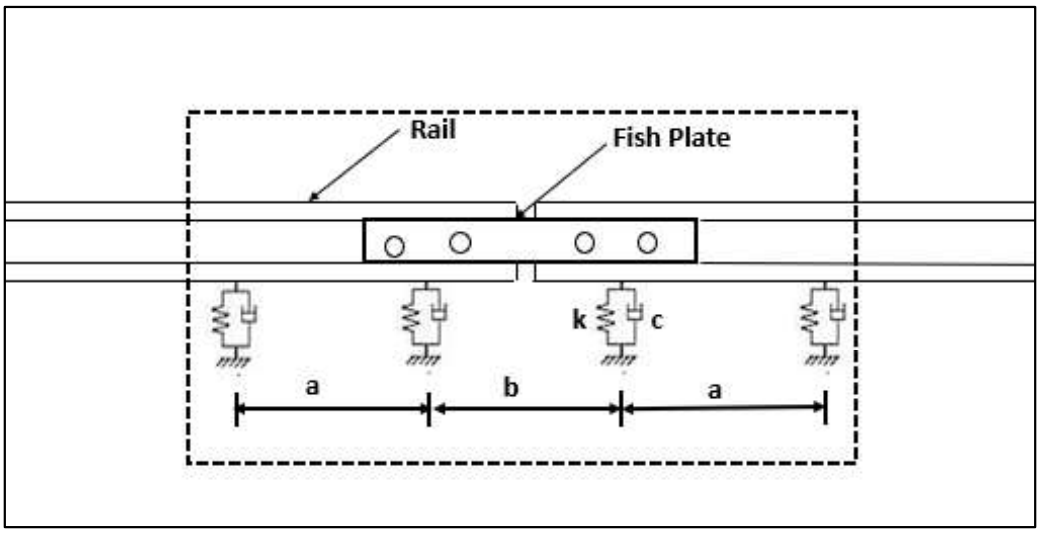

(b)

Fig. 5 Mechanical Model of railway track at rail joint (a) Full track model (b) section of rail model

As shown in Fig. 2, instead of sleepers, which are used to absorb the vibration of the track, springs are attached to the base of rails having longitudinal stiffness(k) and longitudinal damping(c) (Cai et al. 2007). Table 1 shows the detail of joint parameters shown in Fig. 2(b) considered for the simulation.

Table 2. Parameters used in modelling of track model (Cai et al. 2007).

Parameters	L	a	b	d	c	k
Values	12190 mm	610 mm	606 mm	6 mm	14.4 N.s/mm	30700 N/mm

Fig. 8 shows the excitation force profile which is applied at one rail and deflection is calculated on another rail. In this model, the simulation is done with ends of rails taken as free and fixed. Then compare the values of deflection on other side of rail for both the conditions. The simulation is done for 2 different models having different number of rails i.e., 6 and 10. Then compare the difference between the values of deflection on other side of rails for both the end conditions.

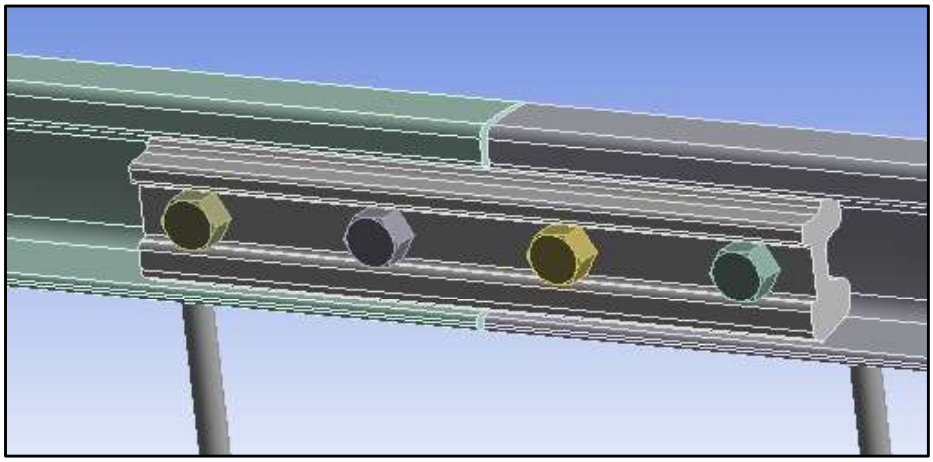

Fig. 6 Contact region at rail joint

The contacts between the plate and the beam is provided in setup. The springs and damper system are used in place of sleepers on which railway lines are laid. The spring having stiffness 3.09 x 10^7 N/m and damping 14400 N.s/m. In the meshing module, the model is divided in to small-2 elements known as mesh. The elements used for the model is 8- node tetrahedral element. The number of nodes and elements changes for different models. For 6-rail model, number of nodes and elements are 503635 and 268347 respectively and for 10-rail model, number of nodes and elements are 847872 and 451033 respectively.

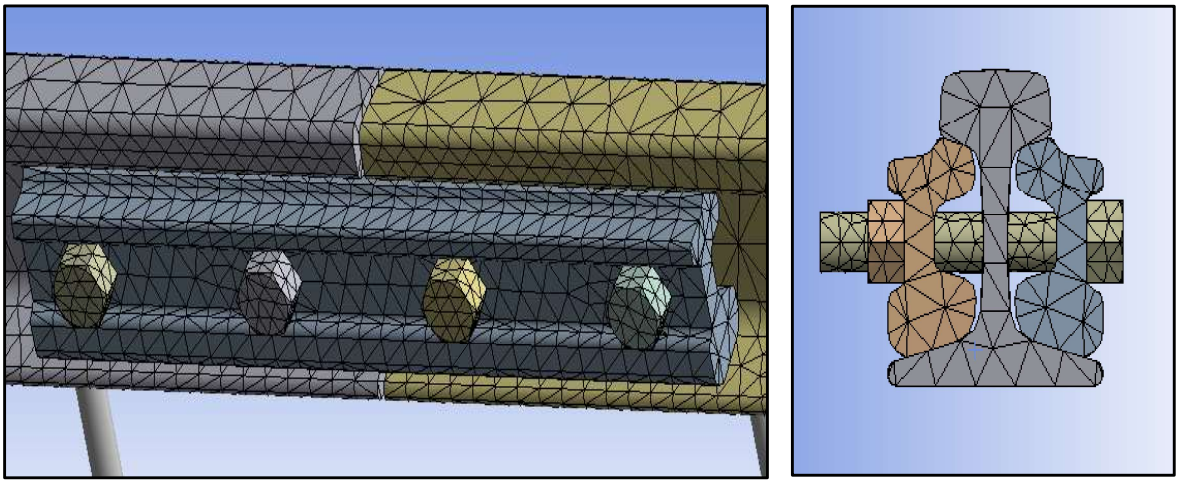

(a) (b)

Fig.7 Meshing of the rail model (a) Meshing of rail joint region (b) Side view of meshed model.

The size of elements is taken as 60 mm for rail tracks and fish plate whereas, for nuts and bolts size of elements are 20 mm. Fine mesh is considered for contact region where size of elements is given 20 mm. On the other hand, in long rails there is no need of fine meshing hence, coarse mesh is sufficient for obtaining good results. Different constraints have been provided to the model such as supports, displacement, force etc. In this model, the end conditions are taken as fixed or free. Remote displacement is used to constraint the displacement of model in any specific direction. Remote displacement provides degree of freedom to the system that in which direction model can translate or rotate.

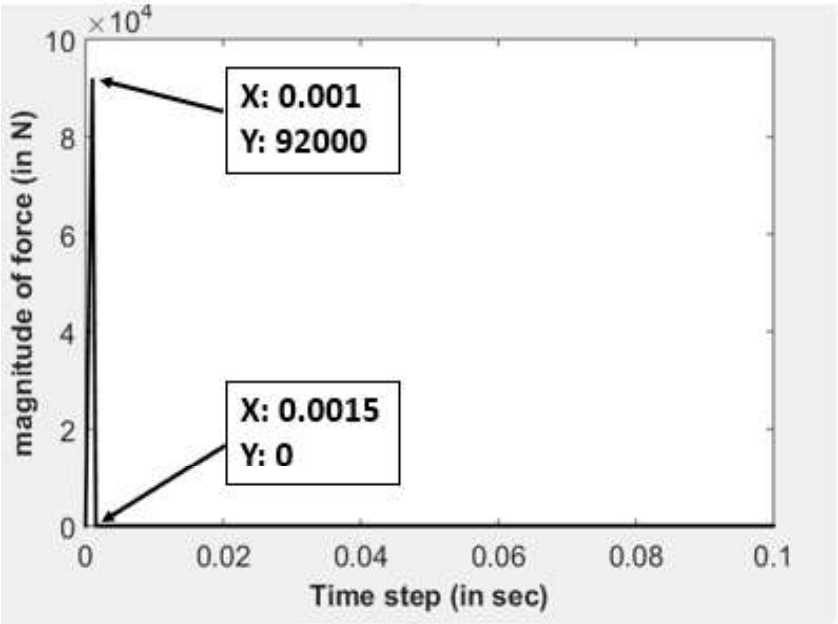

Fig. 8 Impulse force applied to the model

Impact force is assigned at any point in tabular form. Fig. 8 shows the impact force of 92000 N for 0.0001 seconds and at the next time step it is zero. A three-dimensional model of railway track structure is simulated in ANSYS Workbench. The impulse force is applied at the end of first rail. These models are shown in the Fig. 9 and 10 below. 2 models of different lengths have been modelled having end conditions free or fixed.

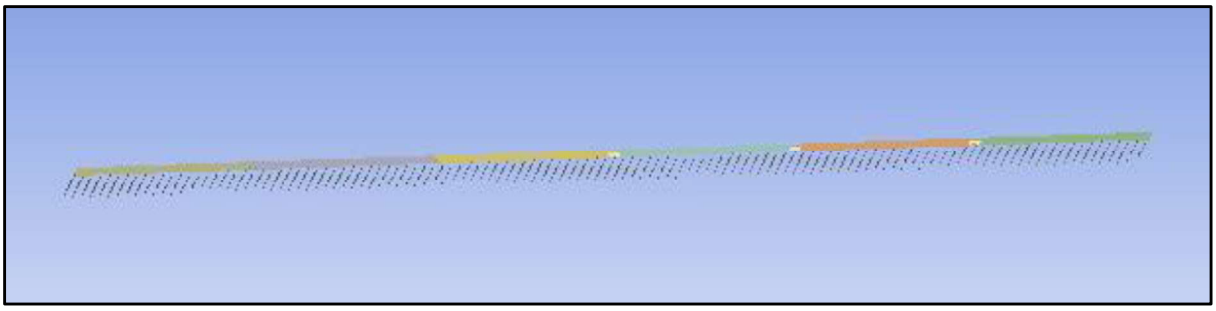

Fig.9 Structural analysis model of 6-rail

Fig.9 shows the 6-rail model simulated in the Ansys Workbench. Spring and damper system is used in place of sleeper providing same stiffness as in sleepers. As shown in the Fig. 10, 10-rail model is also modelled for both boundary conditions. A fish plate is modelled between the rails to join them.

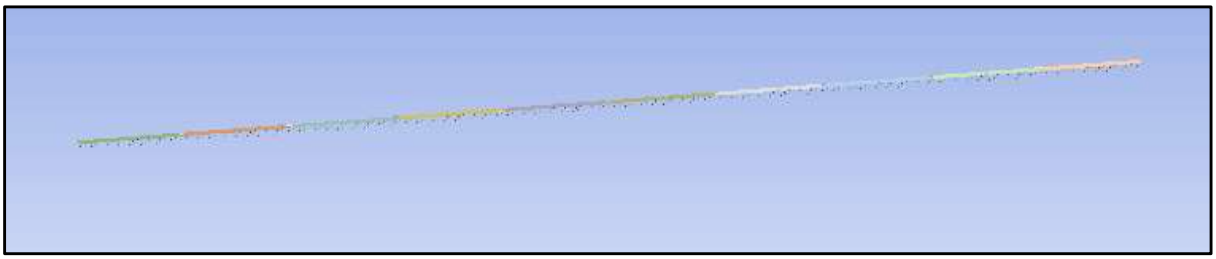

Fig.10 Structural analysis model of 10-rail

3.3 Basic validation of numerical test model

Before starting the actual numerical study, a preliminary validation of the test model has been carried out. For the validation a small experiment setup has been made in which an equivalent model of a rail with a joint is realised using the two beams along with the number of spring joints. In this validation, only the accuracy of the model has been checked by measuring the natural frequency of the model. A small-scale model of railway track is modelled in which two rails are vertically attached to the sleeper with nut and bolts. A joint is used to join these two rails with the help of nut and bolts. Stiffness of sleepers in this model is calculated by putting

1.8 Kg of mass at its free end. The stiffness measured is 6500 N/m. An Accelerometer is the device which is used to measure the vibration signal. Accelerometer used in this experiment has sensitivity 9.926 mV/g. It is attached to the NI-DAQ card which is used to plot the data in the software named LabVIEW. LabVIEW receives all the data of accelerometer through DAQ card and waveform is generated in the software. The waveform data is then exported to excel file to get the desired output. An Oscilloscope can also be used to measure the accelerometer data.

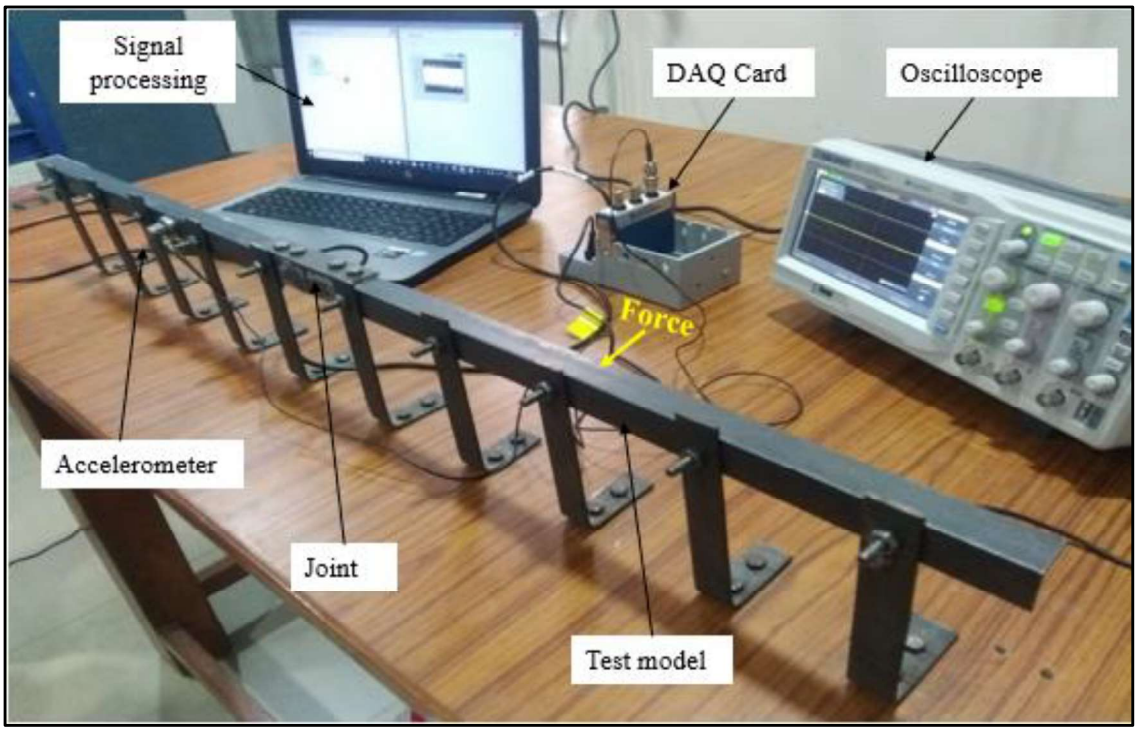

Fig.11 Test model setup with the instruments

A model was also made in the ANSYS having same cross section for verifying the results with the experimental data. Modal analysis has been done in the Ansys to find out the natural frequency of the model and then validate the model with the experimental data. In place of sleepers, springs having stiffness 6500N/mm is used. Hence, this experiment also verifies the use of springs instead of the sleepers in the analysis.

First, model is developed in design modeller and assigned the structural steel as a material. Meshing has been done in the mechanical solver while assigning contact between joint and rails and providing springs in the model. Natural frequency for different mode is then measured. Meshed model generated is shown in the Fig.12 (a) and the joint mesh is shown in Fig. 12(b)

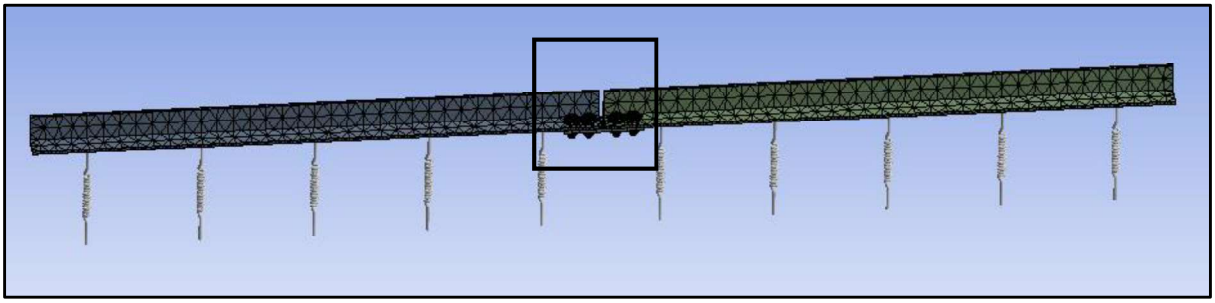

(a)

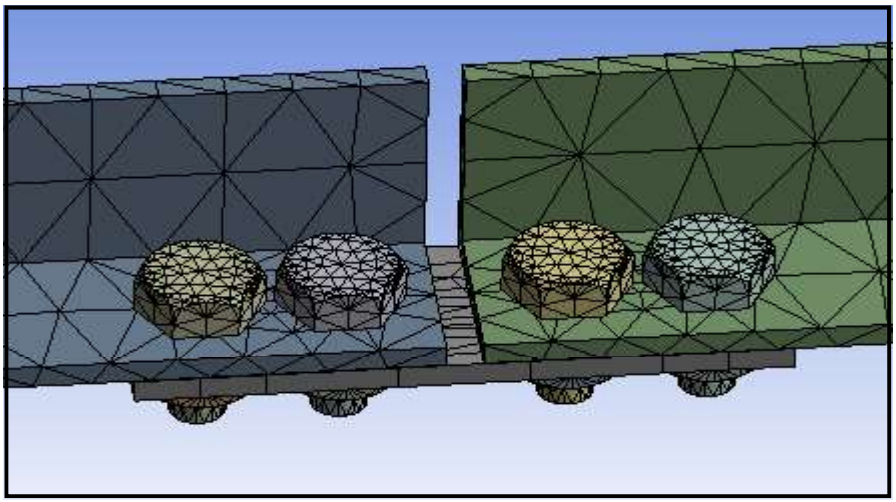

(b)

Fig.12 Design of test model (a) meshing of full test model (b) meshing at joint region

The natural frequency of test model is validated in modal analysis in which different mode shape is obtained. For vertical displacement, 1st mode shape obtained is of 38.051 Hz as shown in the Fig.13. The natural frequency obtained from modal analysis is very close to the natural frequency obtained from the experimental results.

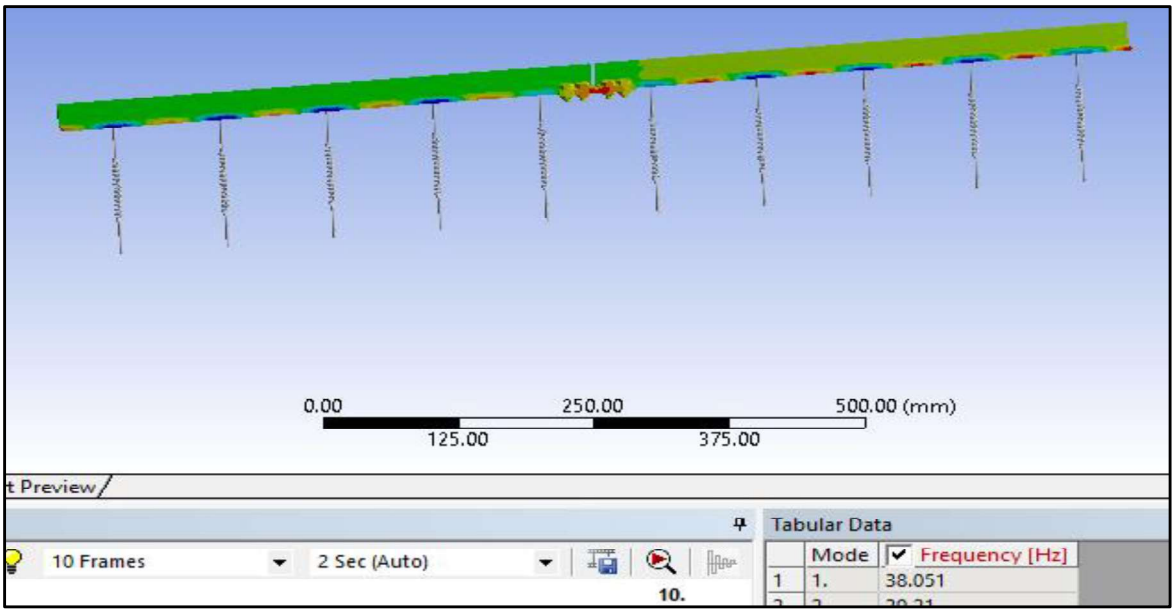

Fig. 13 Mode shape of test model at 1st mode

Fig. 14 shows the plot which is obtained from the test model when impact force is applied on it. As shown in the Fig. 14, multiple frequencies were obtained from the graph so, we have to calculate fft of this signal. MATLAB code is used for finding the natural frequency of the test model.

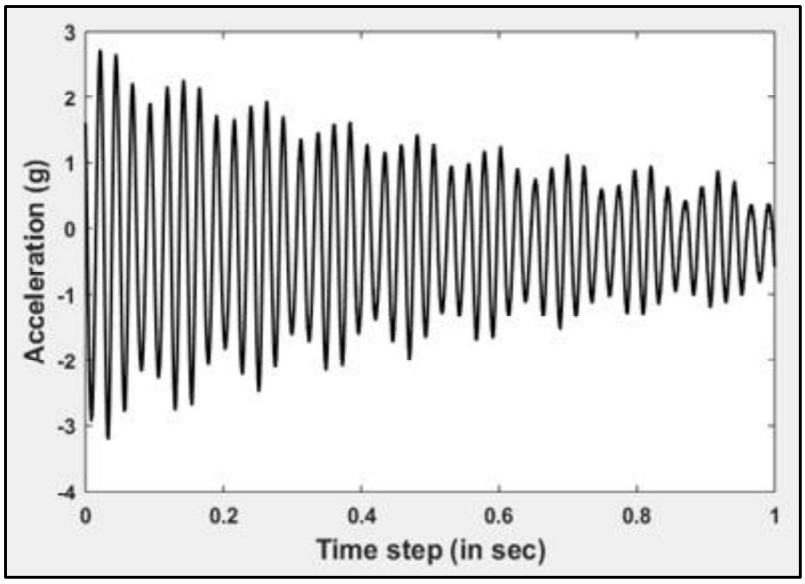

Fig. 14 Response calculated from test model

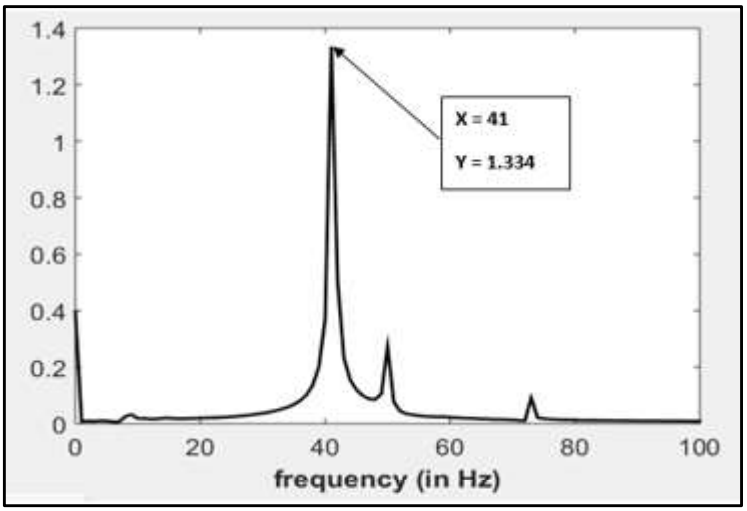

Fig.15 Natural frequency of test model

Fig. 15 shows the Fourier transform of the signal which shows that the natural frequency of the test model is 41 Hz, which is close to the frequency obtained from the modal analysis. The variation in the experimental and numerical study may be due to pretension effect in the bolted joint in the test rig. Nevertheless, from the results obtained, it can be concluded that Numerical model is suitable for a dynamic analysis of rail track.

CHAPTER 4

RESULTS AND DISCUSSION

In the study of vibration propagation characteristics of a rail, it is also important to identify the role of joint connections. In the present work, two models of 6 rails and 10 rails connected with fish plate joints are dynamically analysed. To understand the role of end boundary, both free and fixed end boundary conditions are employed in the investigation. In all the cases an impulsive force of 92000N has been applied at one end of the rail 1.

4.1 Response of 6 rails model

Response of the 6 rails model, as shown in Fig. 16 for an impulsive load is now presented. The ends of the rails are modelled as free boundary condition. Table 3 shows the amplitude of vibration at different points in the 6-rail model.

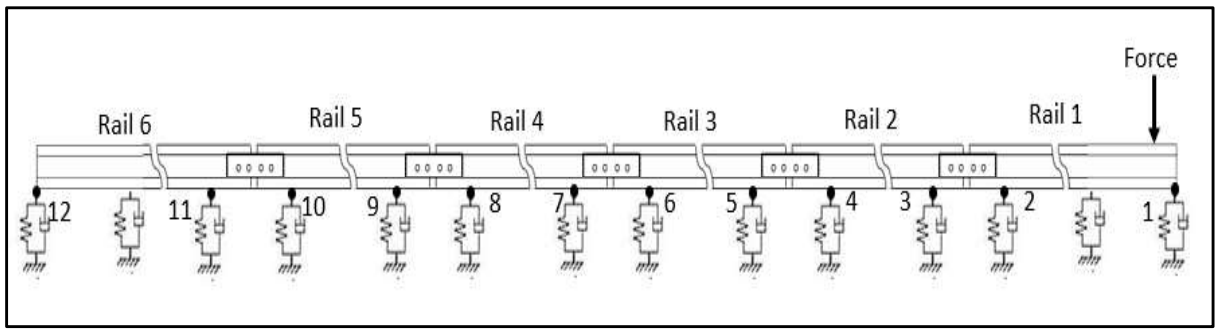

Fig.16 6-rail model

The results from simulation is presented when rail end is taken as free. Fig. 17, 18 and 19 shows the graph at point 1,2 and 3 respectively, on the 6-rail model having boundary conditions free.

It is shown in these graphs that amplitude of vibration signal decays as it travels along the rail. Fig.18 and 19 shows the decay in amplitude when vibration is transmitted through fish plate joint.

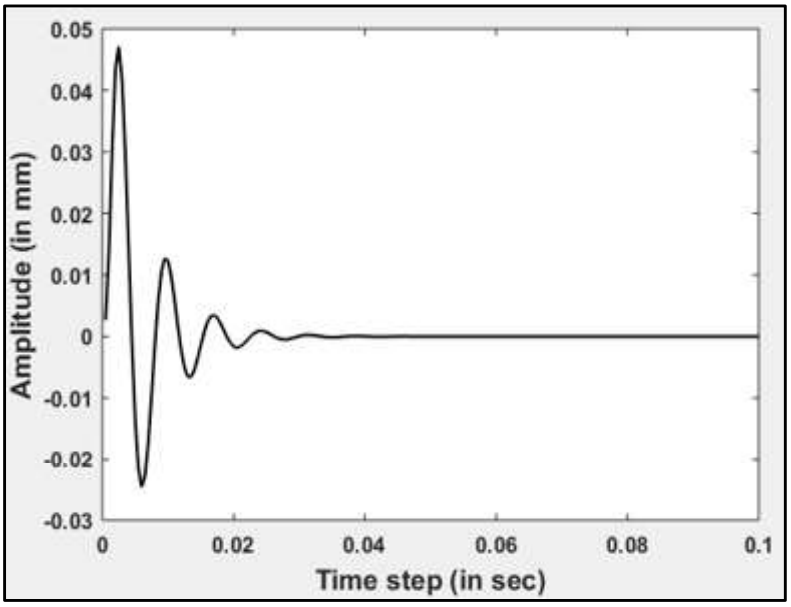

Fig. 17 Amplitude at point 1 on 6-rail model with free boundary conditions.

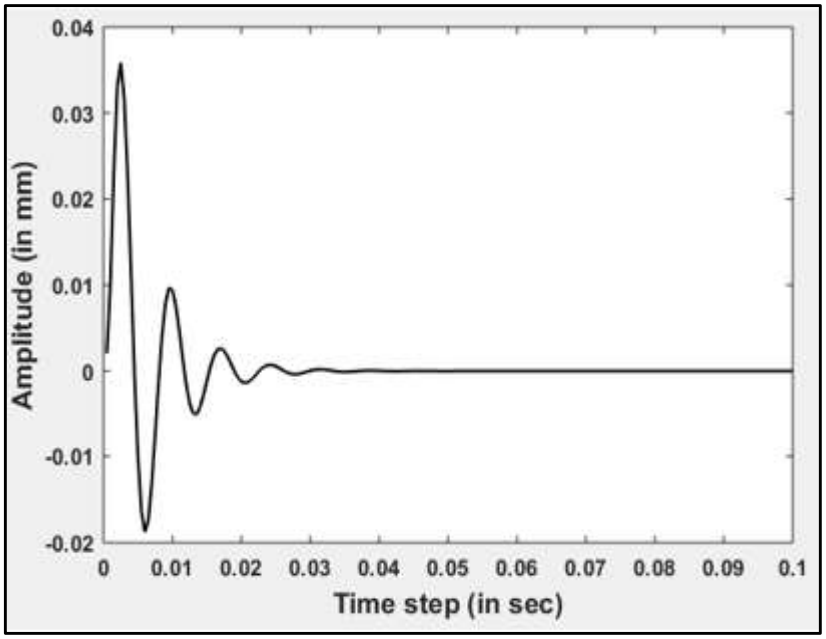

Fig.18 Amplitude at point 2 on 6-rail model with free boundary conditions.

As shown in the Fig. 17 and 18, the difference in the amplitude of vibration signal is 0.0113 mm and when signal transmits from the fish plate joint as shown in Fig 18 and 19, the decay in the amplitude of signal is 0.0006 mm and is very small.

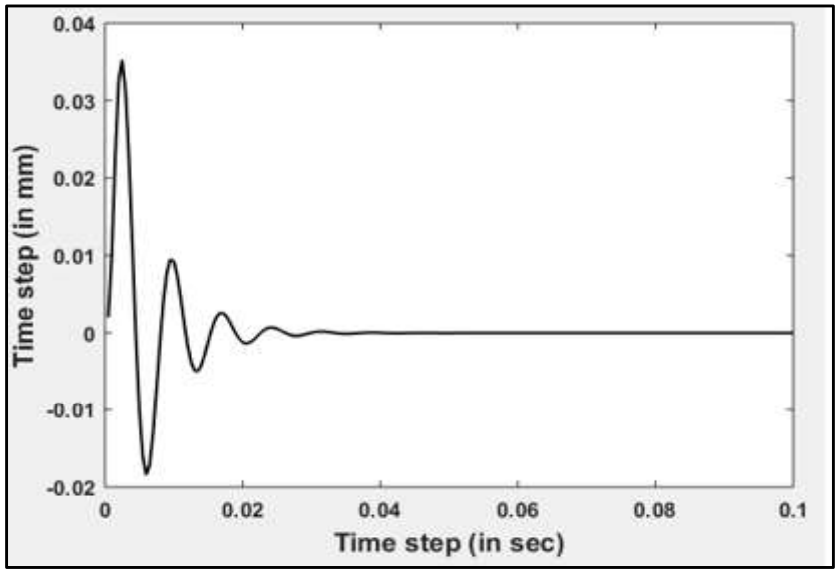

Fig. 19 Amplitude at point 3 on 6-rail model with free boundary conditions.

Table 3: Decay in 6-rail model for free boundary conditions:

Points	Amplitude (mm)	Points	Amplitude Decay (mm)	Percentage Decay (%)	Decay per meter Length (mm)
1.	0.0471	**1-2**	0.0113	23.99%	0.0009
2.	0.0358	**2-3**	0.0006	1.6%	
3.	0.0352	**3-4**	0.0112	31.81%	0.0009
4.	0.0240	**4-5**	0.0006	2.5%	
5.	0.0234	**5-6**	0.0113	48.29%	0.0009
6.	0.0121	**6-7**	0.0006	4.9%	
7.	0.0115	**7-8**	0.0073	63.47%	0.0006
8.	0.0042	**8-9**	0.0006	14.4%	
9.	0.0036	**9-10**	-0.0024	increased	increased
10.	0.0060	**10-11**	-0.0003		
11.	0.0063	**11-12**	-0.0058		
12.	0.0121				

As shown in the table, it can be seen that amplitude of vibration continuously decreasing till the 7th point and then increasing. The increase in the signal may be due to the free end of the track model. For identify the role of a joint in the track, amplitude of vibration is measured at both sides of the joint, which is used to calculate the decay due to the joint.

It may be noted that change in displacement amplitude from point 2 to 3 is 0.0006 mm, which is very close to the decay measured for the pairs of points 4-5, 6-7 and 8-9. These results show that the decay of the level of vibration is negligible as compared to the vibration signal passing through the joint. Fig. 20 shows the decay in the vibration amplitude when the rail ends are taken as free. From the figure, it is observed that the vibration signal decays till the point 5 and then it starts increasing. It is expected that the increase in the vibration amplitude is due to the free end of rail.

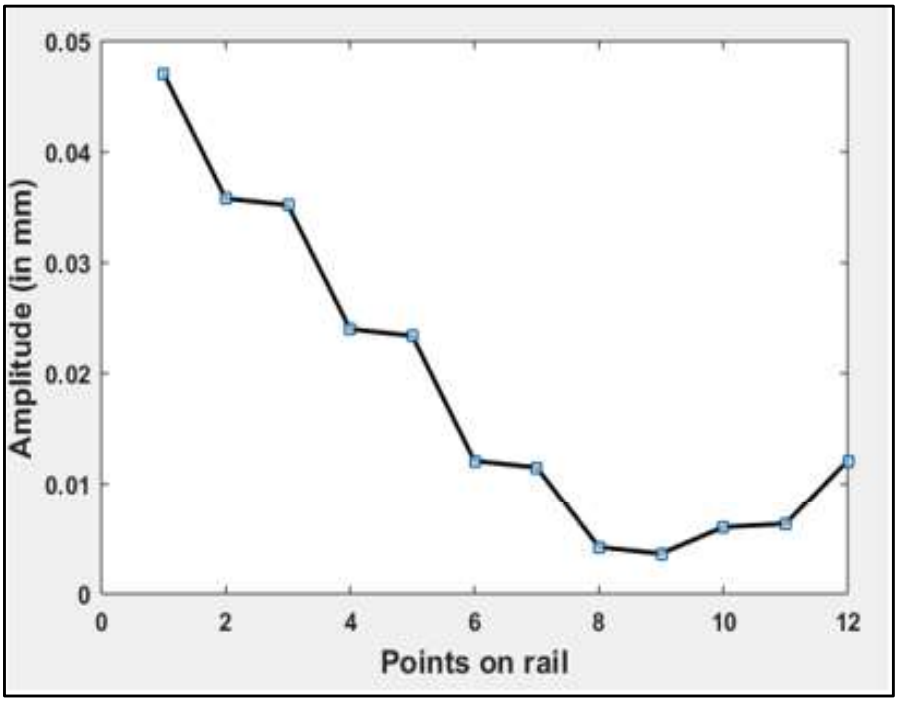

Fig. 20 Decay in amplitude in 10-rail model when end of rails are free

To check the effect of the end boundary, the ends of the rails are modelled as fixed boundary

condition. Fig. 21, 22 and 23 shows the graph at point 1,2 and 3 respectively, on the 6-rail model having boundary conditions fixed. It is shown in these graphs that amplitude of vibration signal decays as it travels along the rail. Fig. 22 and 23 shows the decay in amplitude when vibration is transmitted through fish plate joint.

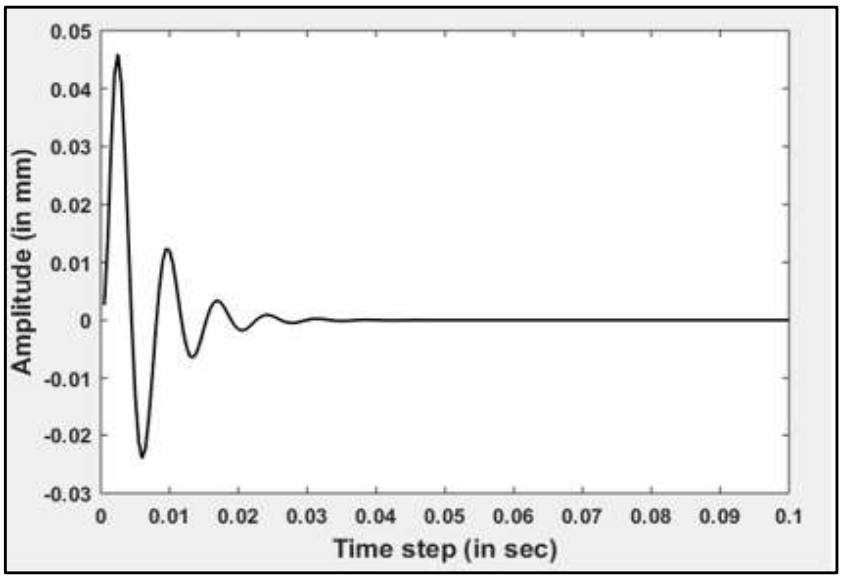

Fig. 21 Amplitude at point 1 on 6-rail model with fixed boundary conditions.

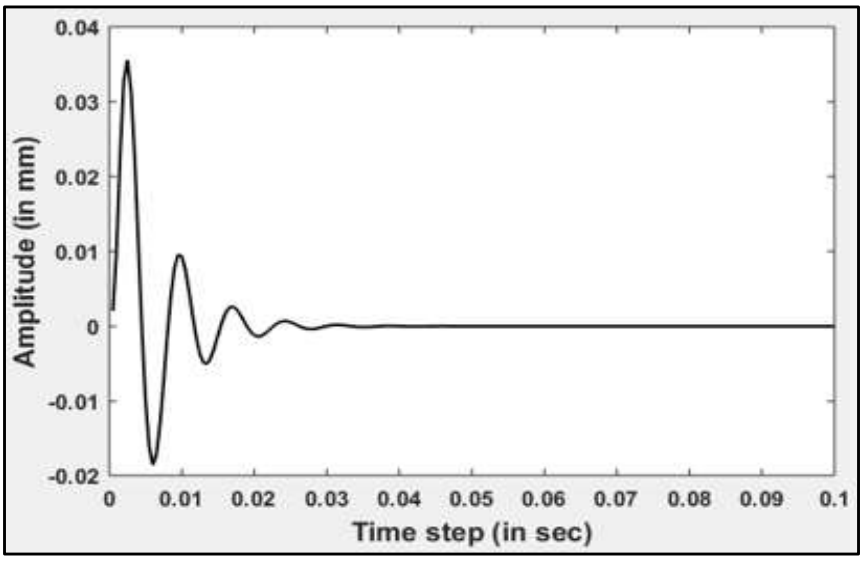

Fig. 22 Amplitude at point 2 on 6-rail model with fixed boundary conditions.

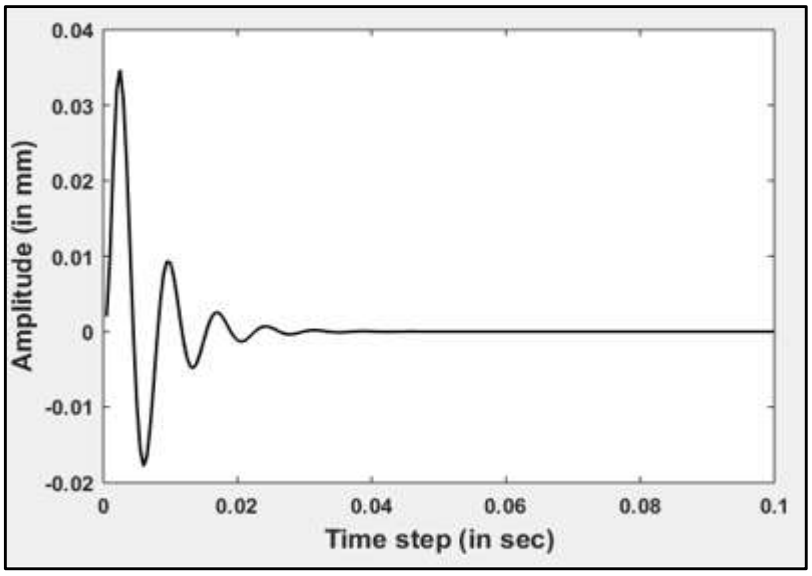

Fig. 23 Amplitude at point 3 on 6-rail model with fixed boundary conditions.

As shown in the Table 4, it can be seen that amplitude of vibration continuously decreasing till the 7th point and then increasing a bit before coming back to zero. For identify the role of a joint in the track, amplitude of vibration is measured at both sides of the joint, which is used to calculate the decay due to the joint.

Table 4: Decay in 6-rail model for fixed boundary conditions

Points	**Amplitude (mm)**	**Points**	**Amplitude Decay (mm)**	**Percentage Decay (%)**	**Decay per meter Length (mm)**
1.	0.0464	**1-2**	0.0109	23.49%	0.0009
2.	0.0355	**2-3**	0.0006	1.6%	
3.	0.0349	**3-4**	0.011	31.51%	0.0009
4.	0.0239	**4-5**	0.0005	2.09%	
5.	0.0234	**5-6**	0.011	47%	0.0009
6.	0.0124	**6-7**	0.0006	4.8%	
7.	0.0118	**7-8**	-0.011	Increased	increased
8.	0.0228	**8-9**	-0.0006		
9.	0.0234	**9-10**	-0.0016		
10.	0.025	**10-11**	-0.0006		
11.	0.0256	**11-12**	0.0256		
12.	0				

It may be noted that change in displacement amplitude from point 2 to 3 is 0.0006 mm, which is very close to the decay measured for the pairs of points 4-5, 6-7 and 8-9. These results show that the decay of the level of vibration is negligible as compared to the vibration signal passing through the joint. Fig. 24 shows the decay in the vibration amplitude when the rail ends are taken as fixed. From the figure, it is observed that the vibration signal decays continuously till the 7th point, then increases suddenly before coming to zero.

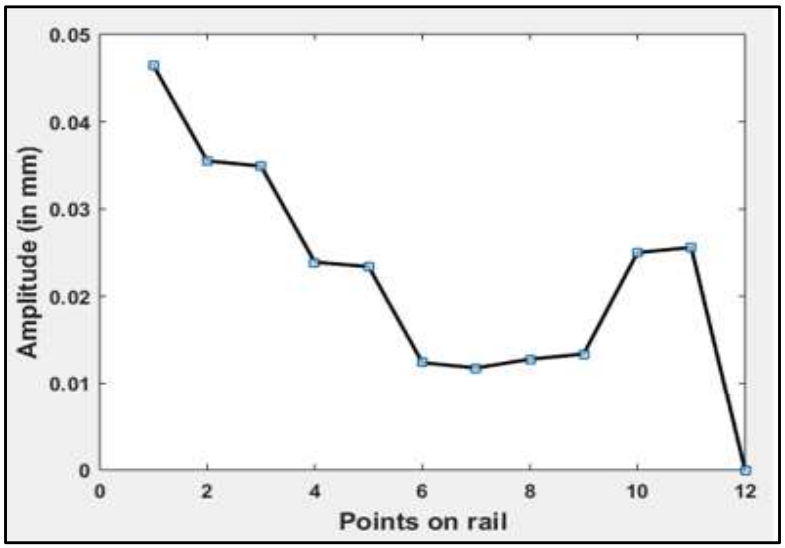

Fig. 24 Decay in amplitude in 10-rail model when end of rail is fixed

4.2 Response of 10 rails model

A similar study is also carried out for a test model of 10 rails. Response of the 10 rails model, as shown in Fig. 25 for an impulsive load is now presented.

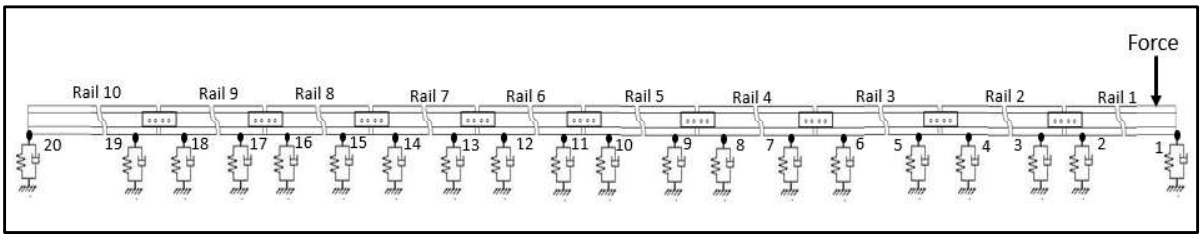

Fig.25 10-rail model

The ends of the rails are modelled as free boundary condition. Table 5 shows the amplitude of vibration at different points Fig. 26, 27 and 28 shows the graph at point 1,2 and 3 respectively, on the 10-rail model having boundary conditions free. It is shown in these graphs that amplitude of vibration signal decays as it travels along the rail. Fig.27 and 28 shows the decay in amplitude when vibration is transmitted through fish plate joint.

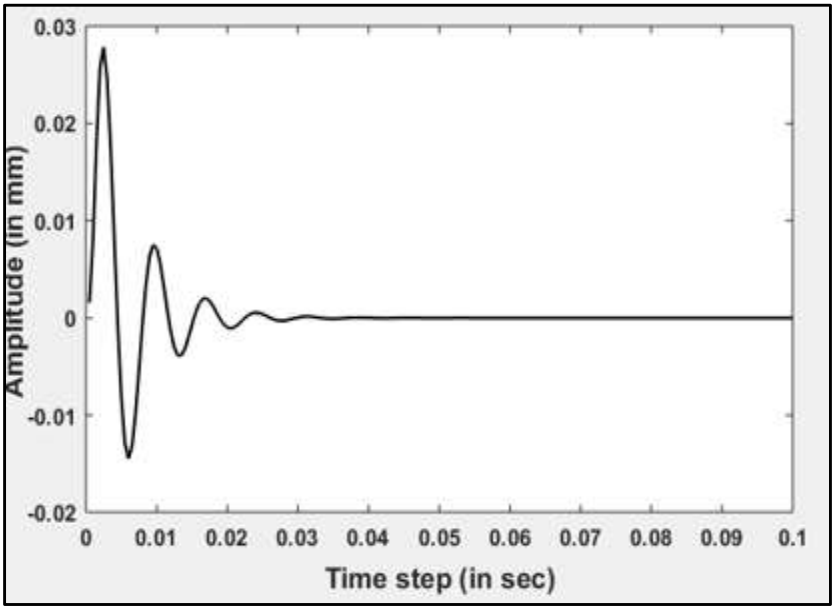

Fig. 26 Amplitude at point 1 on 10-rail model with free boundary conditions.

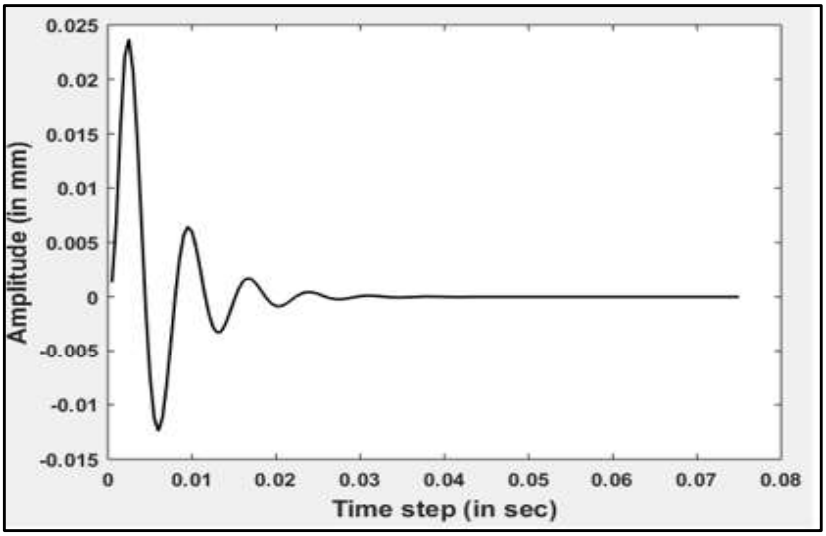

Fig. 27 Amplitude at point 2 on 10-rail model with free boundary conditions

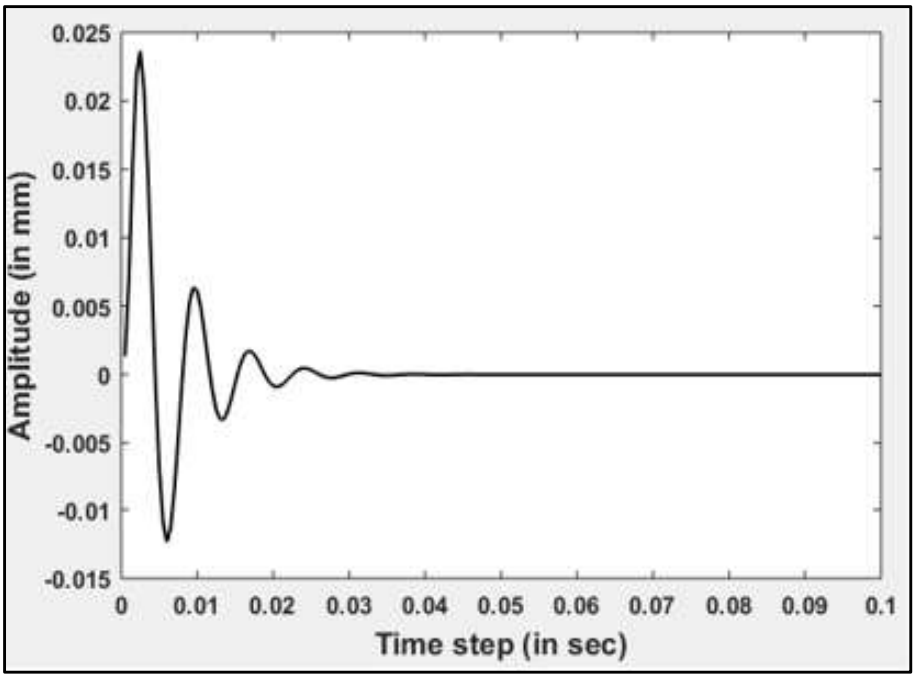

Fig. 28 Amplitude at point 3 on 10-rail model with free boundary conditions

As shown in the Table 5, it can be seen that amplitude of vibration continuously decreasing till the 14th point and then increasing. The increase in the signal may be due to the free end of the track model. For identify the role of a joint in the track, amplitude of vibration is measured at both sides of the joint, which is used to calculate the decay due to the joint. As shown in the Table 5, the results of 10-rail model also assure that there is not much decay in the vibration signal when it passes through the signal. The decay in the signal is mainly due to the stiffness and damping of the sleepers. As in 10-rail model, when signal passes through joint from point 2-3, 4-5, 6-7, 8-9, 10-11 and 12-13, the difference in amplitude is 0.0002mm which denotes that there is not much role of fish plate joint in decaying the vibration signal. The decay per metre length is 0.0003mm. It can be seen that decay in the vibration. Fig. 29 shows the decay in the vibration amplitude when the rail ends are taken as free. From the figure, it is observed that the vibration signal decays till the point 14 and then it starts increasing

Table5: Decay in 10-rail model for free boundary condition:

Points	Amplitude (mm)
1.	0.0278
2.	0.0238
3.	0.0236
4.	0.0196
5.	0.0194
6.	0.0154
7.	0.0152
8.	0.0112
9.	0.0110
10.	0.0070
11.	0.0068
12.	0.0028
13.	0.0026
14.	0.0007
15.	0.0008
16.	0.0028
17.	0.0030
18.	0.0050
19.	0.0051
20.	0.0072

Points	Amplitude Decay (mm)	Percentage Decay (%)	Decay per meter Length (mm)
1-2	0.004	14.3%	0.0003
2-3	0.0002	0.84%	
3-4	0.004	16.9%	0.0003
4-5	0.0002	1.02%	
5-6	0.004	20.61%	0.0003
6-7	0.0002	1.2%	
7-8	0.004	26.31%	0.0003
8-9	0.0002	1.7%	
9-10	0.004	36.36%	0.0003
10-11	0.0002	2.8%	
11-12	0.004	58.82%	0.0003
12-13	0.0002	7.1%	
13-14	0.0019	73.07%	0.0003
14-15	-0.0001	increasing	increasing
15-16	-0.002		
16-17	-0.0002		
17-18	-0.002		
18-19	-0.0001		
19-20	0.0021		

.

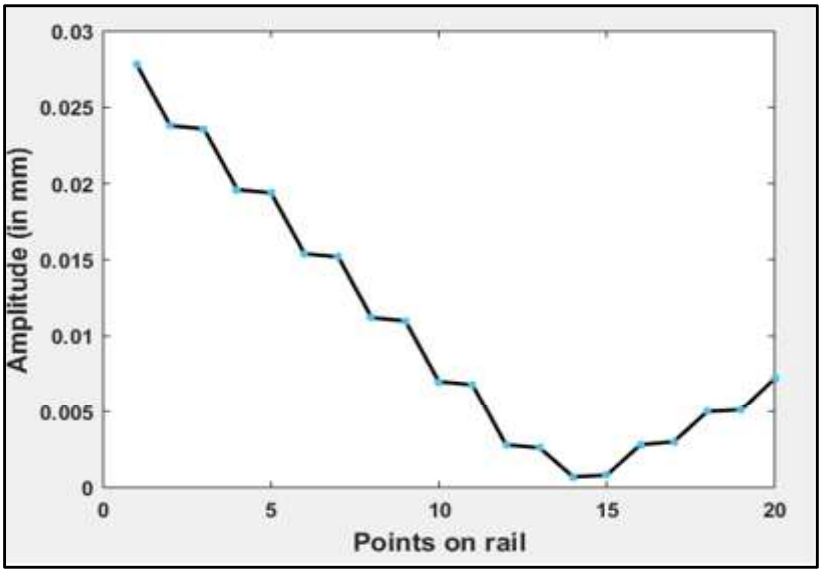

Fig. 29 Decay in amplitude in 10-rail model when end of rails are free

Fig. 29 shows the decay in the vibration amplitude when the rail ends are taken as free. From the figure, it is observed that the vibration signal decays till the point 14 and then it starts increasing. It is expected that the increase in the vibration amplitude is due to the free end of rail. To check the effect of the end boundary, the ends of the rails are modelled as fixed boundary condition. Fig. 30, 31 and 32 shows the graph at point 1,2 and 3 respectively, on the 10-rail model having boundary conditions fixed. It is shown in these graphs that amplitude of vibration signal decays as it travels along the rail. Fig. 31 and 32 shows the decay in amplitude when vibration is transmitted through fish plate joint.

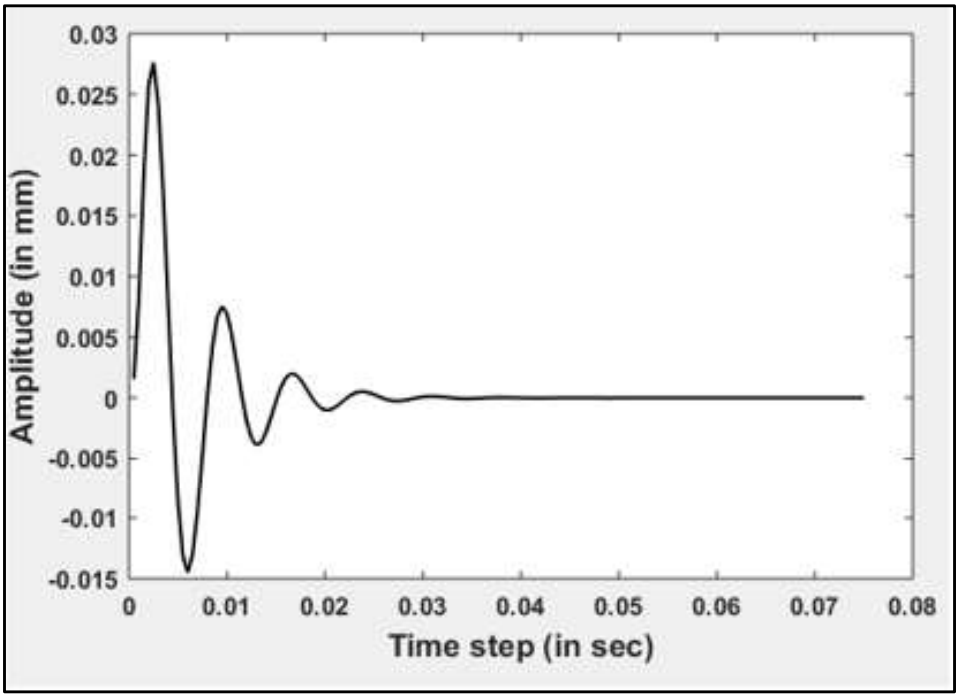

Fig. 30 Amplitude at point 1 on 10-rail model with fixed boundary conditions

The decay in the amplitude of vibration signal is almost same in all the rails. There is not much difference in the decay of vibration signal in the fish plate, hence it may not affect the vibration transmission and can be neglected.

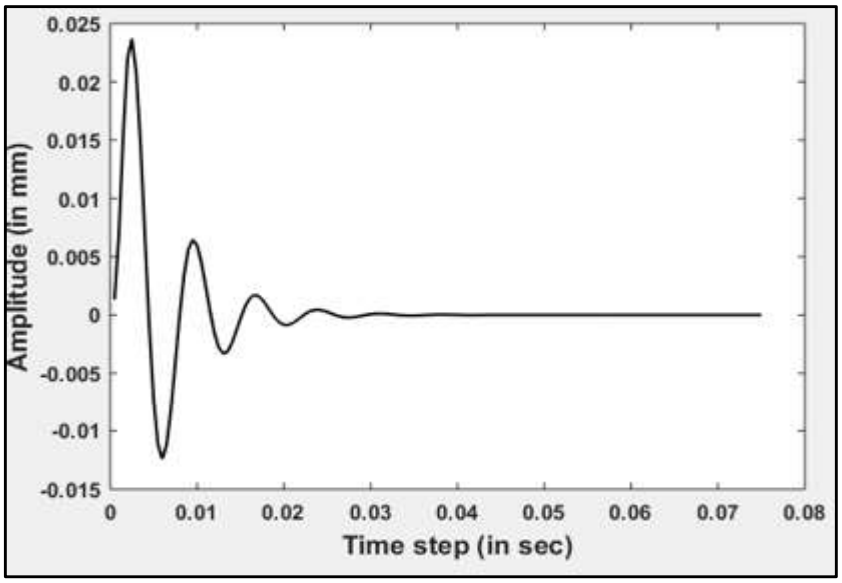

Fig. 31 Amplitude at point 2 on 10-rail model with fixed boundary conditions

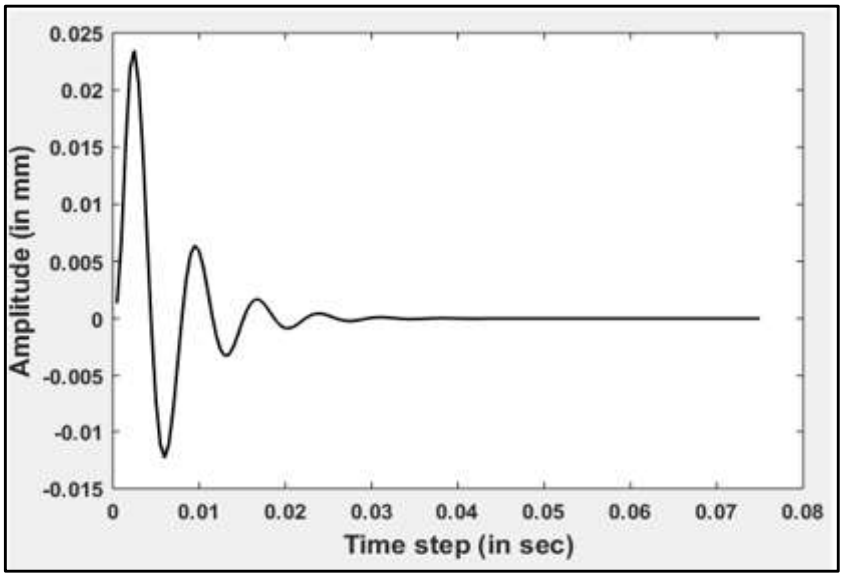

Fig.32 Amplitude at point 3 on 10-rail model with fixed boundary conditions

As shown in the Table 6, it can be seen that amplitude of vibration continuously decreasing till the 14th point and then increasing. For identify the role of a joint in the track, amplitude of vibration is measured at both sides of the joint, which is used to calculate the decay due to the joint. As shown in the Table 6, the results of 10-rail model for fixed end, also assure that there is not much decay in the vibration signal when it passes through the signal. The decay in the

signal is mainly due to the stiffness and damping of the sleepers. As in 10-rail model, when signal passes through joint from point 2-3, 4-5, 6-7, 8-9, 10-11 and 12-13, the difference in amplitude is 0.0002 mm which denotes that there is not much role of fish plate joint in decaying the vibration signal.

Table6: Decay in 10-rail model for fixed boundary condition:

Points	Amplitude (mm)
1.	0.0276
2.	0.0236
3.	0.0234
4.	0.0195
5.	0.0193
6.	0.0154
7.	0.0152
8.	0.0112
9.	0.0110
10.	0.0071
11.	0.0069
12.	0.0030
13.	0.0028
14.	0.0010
15.	0.0011
16.	0.0030
17.	0.0031
18.	0.0050
19.	0.0051
20.	0

Points	Amplitude Decay (mm)	Percentage Decay (%)	Decay per meter Length (mm)
1-2	0.004	14.3%	0.0003
2-3	0.0002	0.84%	
3-4	0.004	16.9%	0.0003
4-5	0.0002	1.02%	
5-6	0.004	20.61%	0.0003
6-7	0.0002	1.2%	
7-8	0.004	26.31%	0.0003
8-9	0.0002	1.7%	
9-10	0.004	36.36%	0.0003
10-11	0.0002	2.8%	
11-12	0.004	58.82%	0.0003
12-13	0.0002	7.1%	
13-14	0.0019	73.07%	0.0001
14-15	-0.0001	increasing	increasing
15-16	-0.0019		
16-17	-0.0001		
17-18	-0.0019		
18-19	-0.0001		
19-20	0.0051		

From the aforementioned results, it may be inferred that the decay of vibration signal in the joint is relatively small. The signal decays in case of the 10-rail model when end of rail is fixed but suddenly rises before coming to zero as shown in the Fig. 33. It indicates that in the

estimation of vibration transmission through the rails, the joints can be modelled as simple connection or may be ignored.

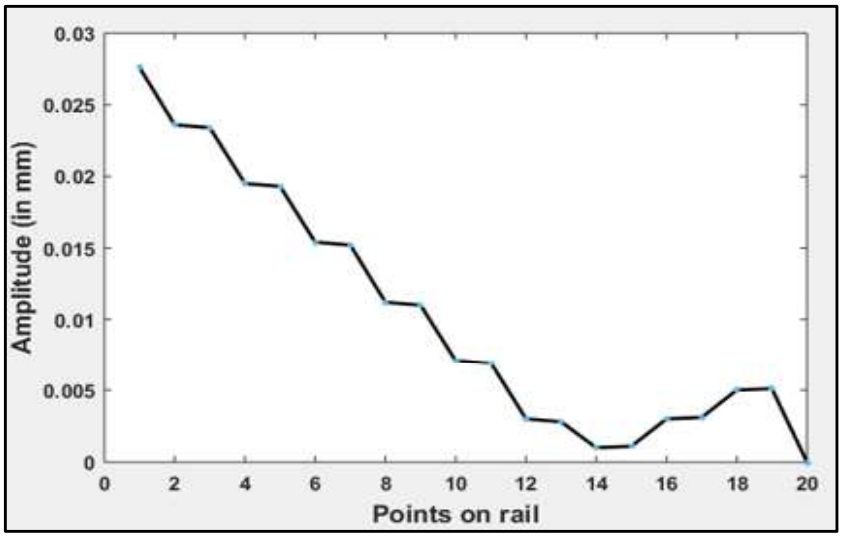

Fig. 33 Decay in amplitude in 10-rail model when end of rail is fixed

From the analysis of decaying of the vibration through the rails, from the case of 10 rails modelled as free end boundary, it is observed that vibration level becomes 80% of its initial value after crossing a distance of approximately 85 meters. The fixed end boundary also shows similar trend. On the other hand, the rate of decay measured from the 6 rails model gives relatively higher decay rate. This contradictory result raises a concern about correct modelling of the track incorporating correct boundary conditions. In the present study, both free and fixed end boundaries are incorporated and analysed, their results are also in good agreement with each other. Nevertheless, prediction of correct distance to design an automated alarming system for an unmanned railway crossing required further investigation, where in the FE model may be required to equip with a continuous end boundary.

CHAPTER 5

CONCLUSIONS AND FUTURE SCOPE

Estimation of vibration carrying characteristics of railway track is important to design an automated signalling mechanism. Such mechanism is useful to alarm at the unmanned crossing spread across our country. In the present work, a dynamic analysis of railway track with fish plate is performed to estimate the transmission of vibration signal from the rails and the fish plate joint. Simulations are performed on a 3-D finite element model using a commercial CAE tool ANSYS Workbench. A small experimental set up is also prepared for the validation of the numerical model used for of the dynamic study. Validation is done by comparing free vibration frequency of the experimental set up and the numerical model. In study of rails with the joints, two rail-models i.e. 6-rail model and 10-rail model have been numerically simulated. Both models have been simulated for two boundary conditions i.e., free end and fixed end. The ends of both the models are first taken as free and then fixed to understand the effect of boundary conditions on the vibration transmission. The following are the conclusions drawn from the present work:

1 It is concluded from the results that decay of vibration signal through fish pate joint is almost negligible and can be neglected for vibration transmission study of railway track.
2 The distance at which vibration signal decays 80% has been calculated as 85 meters.
3 It is noted that study of decay in the vibration signal depends on the boundary condition of the railway track.

Hence, the main objective of the present work has been successfully achieved which is the role of fish plate joint considering vibration transmission characteristics. The distance at

which the vibration signal decay in railway track has been calculated as 85m from numerical simulation. Further experiments on railway tracks are required for better accurate results and validate the results of numerical simulation. Also, the identification of correct boundary conditions for modelling of 3-D model is also important.

REFERENCES

Cai, W., Wen, Z., Jin, X. and Zhai, W., 2007. Dynamic stress analysis of rail joint with height difference defect using finite element method. *Engineering Failure Analysis*, *14*(8), pp.1488-1499.

Chen, Y.C. and Kuang, J.H., 2002. Contact stress variations near the insulated rail joints. *Proceedings of the Institution of Mechanical Engineers, Part F: Journal of Rail and Rapid Transit*, *216*(4), pp.265-273.

Clark, R.A., Dean, P.A., Elkins, J.A. and Newton, S.G., 1982. An investigation into the dynamic effects of railway vehicles running on corrugated rails. *Journal of Mechanical Engineering Science*, *24*(2), pp.65-76.

Dong, R.G., Sankar, S. and Dukkipati, R.V., 1994. A finite element model of railway track and its application to the wheel flat problem. *Proceedings of the Institution of Mechanical Engineers, Part F: Journal of Rail and Rapid Transit*, *208*(1), pp.61-72.

Gallou, M., Temple, B., Hardwick, C., Frost, M. and El-Hamalawi, A., 2018. Potential for external reinforcement of insulated rail joints. *Proceedings of the Institution of Mechanical Engineers, Part F: Journal of Rail and Rapid Transit*, *232*(3), pp.697-708.

Gallou, M., 2018. *The assessment of track deflection and rail joint performance* (Doctoral dissertation, Loughborough University).

Grassie, S.L., Gregory, R.W., Harrison, D. and Johnson, K.L., 1982. The dynamic response of railway track to high frequency vertical excitation. *Journal of Mechanical Engineering Science*, *24*(2), pp.77-90.

Hasna, P.H., 2015. Study of dynamic behavior of rail track using finite element method. *International Journal of Engineering Research and General science*, *3*(6), pp.668-676.

Himebaugh, A.K., Plaut, R.H. and Dillard, D.A., 2008. Finite element analysis of bonded insulated rail joints. *International Journal of Adhesion and Adhesives*, *28*(3), pp.142-150.

Kerr, A.D. and Cox, J.E., 1999. Analysis and tests of boned insulted rail joints subjected to vertical wheel loads. *International Journal of Mechanical Sciences*, *41*(10), pp.1253-1272.

Lal, R., Singh, R.C. and Singh, D., Stress Analysis at Contact Region of Rail-Wheel.

Mandal, N.K. and Peach, B., 2010. An engineering analysis of insulated rail joints: a general perspective. *Int J Eng Sci Technol*, *2*(8), pp.3964-88.

Mandal, N.K., 2014. On the low cycle fatigue failure of insulated rail joints (IRJs). *Engineering Failure Analysis*, *40*, pp.58-74.

Nielsen, J.C., 2008. High-frequency vertical wheel–rail contact forces—Validation of a prediction model by field testing. *Wear*, *265*(9-10), pp.1465-1471.

Ono, K. and Yamada, M., 1989. Analysis of railway track vibration. *Journal of sound and vibration*, *130*(2), pp.269-297.

Oregui, M., Li, Z. and Dollevoet, R.P.B.J., 2012. An investigation into the relation between wheel/rail contact and bolt tightness of rail joints using a dynamic finite element model. In *Proceedings of the 9th International Conference on Contact Mechanics and Wear of Rail/Wheel Systems (CM'12)* (pp. 501-508).

Oregui, M., Molodova, M., Núñez, A., Dollevoet, R.P.B.J. and Li, Z., 2015. Experimental investigation into the condition of insulated rail joints by impact excitation. *Experimental Mechanics*, *55*(9), pp.1597-1612.

Pang, T. and Dhanasekar, M., 2006. Dynamic finite element analysis of the wheel rail interaction adjacent to the insulated rail joints.

Patel, S., Kumar, V. and Nareliya, R., 2013. Fatigue analysis of rail joint using finite element method. *International Journal of Research in Engineering and Technology*, *2*(1), pp.80-84.

Plaut, R.H., Lohse-Busch, H., Eckstein, A., Lambrecht, S. and Dillard, D.A., 2007. Analysis of tapered, adhesively bonded, insulated rail joints. *Proceedings of the Institution of Mechanical Engineers, Part F: Journal of Rail and Rapid Transit*, *221*(2), pp.195-204.

Sandström, J. and Ekberg, A., 2009. Numerical study of the mechanical deterioration of insulated rail joints. *Proceedings of the Institution of Mechanical Engineers, Part F: Journal of Rail and Rapid Transit*, *223*(3), pp.265-273.

Suzuki, T., Ishida, M., Abe, K. And Koro, K., 2005. Measurement on dynamic behaviour of track near rail joints and prediction of track settlement. *Quarterly Report of RTRI*, *46*(2), pp.124-129.

Vyas, N.S. and Gupta, A.K., 2006. Modeling rail wheel-flat dynamics. In *Engineering Asset Management* (pp. 1222-1231). Springer, London.

Wen, Z., Jin, X. and Zhang, W., 2004. Contact-impact stress analysis of rail joint region using the dynamic finite element method. *Wear*, *258*(7-8), pp.1301-1309.

Yang, Z., Boogaard, A., Chen, R., Dollevoet, R. and Li, Z., 2017. Numerical and experimental study of wheel-rail impact vibration and noise generated at an insulated rail joint. *International Journal of Impact Engineering*, *113*, pp.29-39.

Zakeri, J.A. and Xia, H., 2009. Application of 2D-infinite beam elements in dynamic analysis of train-track interaction. *Journal of Mechanical Science and Technology*, *23*(5), pp.1415-1421.

Zong, N., Wexler, D. and Dhanasekar, M., 2013. Structural and material characterisation of insulated rail joints. *Electronic Journal of Structural Engineering*, *13*(1), pp.75-87.

Zong, N. and Dhanasekar, M., 2017. Sleeper embedded insulated rail joints for minimising the number of modes of failure. *Engineering Failure Analysis*, *76*, pp.27-43.